Quantum waveguide theory of the Josephson effect in multiband superconductors

C. Nappi,[1,*] F. Romeo,[2,†] E. Sarnelli,[1] and R. Citro[2,3]

[1]*Consiglio Nazionale delle Ricerche, Istituto Superconduttori, Materiali Innovativi e Dispositivi (CNR-SPIN), Sezione di Napoli, I-80078 Pozzuoli, Napoli (NA), Italy*

[2]*Dipartimento di Fisica "E. R. Caianiello", Università di Salerno, I-84084 Fisciano, Salerno (SA), Italy*

[3]*Consiglio Nazionale delle Ricerche, Istituto Superconduttori, Materiali Innovativi e Dispositivi (CNR-SPIN), Sezione di Salerno, I-84084 Fisciano, Salerno (SA), Italy*

(Received 24 July 2015; revised manuscript received 12 October 2015; published 4 December 2015)

We formulate a quantum waveguide theory of the Josephson effect in multiband superconductors, with special emphasis on iron-based materials. By generalizing the boundary conditions of the scattering problem, we first determine the Andreev levels spectrum and then derive an explicit expression for the Josephson current which generalizes the formula of the single-band case. In deriving the results, we provide a second quantization field theory, allowing us to evaluate the current-phase relation and the Josephson current fluctuations in multiband systems. We present results for two different order parameter symmetries, namely $s_{\pm}$ and s_{++}, which are relevant in multiband systems. The obtained results show that the $s_{\pm}$ symmetry can support π states which are absent in the s_{++} case. We also argue that there is a certain fragility of the Josephson current against phase fluctuations in the s_{++} case. The temperature dependence of the Josephson critical current is also analyzed and we find, for both the order parameter symmetries, remarkable violations of the Ambegaokar-Baratoff relation. The results are relevant in view of possible experiments aimed at investigating the order parameter symmetry of multiband superconductors using mesoscopic Josephson junctions.

DOI: 10.1103/PhysRevB.92.224503 PACS number(s): 74.45.+c, 74.50.+r, 74.70.Xa, 85.25.Cp

I. INTRODUCTION

Multiband superconductivity [1] was theoretically suggested a few years after the BCS formulation of the superconducting state [2]. The discovery of superconductivity in MgB_2 [3] in 2001 and the observation of superconductivity in Fe-based compounds (FeBS) [4,5] in 2008 renewed the interest towards multiband superconductivity. One main goal is understanding the pairing symmetry in this class of superconductors, which is still the object of intensive investigation. In the case of MgB_2 there is a clear consensus towards the picture of two coexisting in-phase superconducting gaps (s_{++} pairing) [6], while in FeBS the experimental evidence seems to favor, in some cases, the $s_{\pm}$ pairing, implying that both the electron-like and the hole-like bands develop an s-wave superconducting state with order parameters of opposite sign [7]. Thus, in the $s_{\pm}$ symmetry, the superconducting gap exhibits a sign reversal between α and β bands which is absent in the s_{++} symmetry. This phase difference can be probed using point contact Andreev reflection spectroscopy (PCARS), which is considered to be one of the high-resolution phase-sensitive techniques to investigate the superconducting order parameter [8–11]. This technique has recently been applied to gain insight on the properties of the FeBS [12,13]. However, in contrast to the high-T_c cuprate superconductivity manifesting a d-wave symmetry, phase sensitive experiments appear to be difficult in FeBS since the s_{++} and $s_{\pm}$ pairings have the same crystallographic symmetry; so far no experiment has been decisive in discriminating between the two symmetries. A complementary tool to gain information on the symmetry of the order parameter is the current-phase relation (CPR) of the Josephson current. In fact, along with PCARS, the Josephson effect has been used in the past as a probe of electronic properties in superconductors, including the order parameter symmetry (see, e.g., Refs. [14–17]).

In this paper we develop a quantum waveguide approach to describe the Josephson effect in a multiband superconducting junction. The model can be used for discriminating between different symmetries of the order parameter (s_{++} and $s_{\pm}$). The presence of more than one band in the superconductor implies that extra scattering channels are present at the interface, a physical situation which is analogous to a quantum waveguide theory problem [18,19] as recently suggested by PCARS modeling of a normal-multiband superconductor junction [20]. We evaluate the Josephson current carried by Andreev bound levels and demonstrate that several distinctive features of the $s_{\pm}$ and s_{++} symmetries of the order parameter can be highlighted in the current-phase relation. The results are particularly relevant with respect to the fast progress in nanofabrication techniques [21], which now allow us to explore the Josephson effect in the mesoscopic junction regime, where supercurrent flows through a small number of channels. In this kind of nanometric junction the effect of a different symmetry, $s_{\pm}$ or s_{++}, should emerge, and the experimental results should be easily compared with the basic theory of the Josephson effect in these materials.

The paper is organized as follows. In Sec. II we present the quantum waveguide model of a multiband superconductor coupled to another identical multiband superconductor (symmetrical junction) and derive the spectral equation of the Andreev bound states. In Sec. III we calculate the Josephson current by using a field theory formalism in second quantization. In Sec. IV we discuss the results for the current-phase relation and the temperature dependence of the critical current. In Sec. V we draw the conclusions. Details on the computation of the scattering coefficients are reported in Appendix A. The theory

*ciro.nappi@spin.cnr.it
†fromeo@sa.infn.it

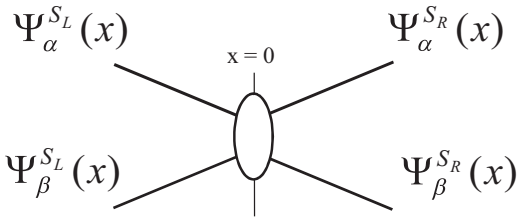

FIG. 1. Quantum waveguide schematization of a two-band Josephson junction. Each branch represents a superconducting band, α or β, in the left (S_L) or right (S_R) electrode. The wave functions of superconducting bands are given by $\Psi_{\alpha,\beta}^{S_L,R}(x)$. The node at $x = 0$ represents the interface between the left and right superconducting banks.

of the magnetic field dependence of the critical current of a Josephson junction is briefly recalled in Appendix B.

II. MODEL AND THEORY

We formulate a ballistic theory of the Josephson effect describing multiband superconducting junctions. The theory allows us to consider an arbitrary number of bands, which are treated as network branches of an effective quantum waveguide model. The proposed approach could be applied to the MgB_2 as well as the FeBS case. In order to develop the theory, hereafter we refer to the specific case of FeBS, for which the s_{++} and $s_{\pm}$ symmetries have been suggested. The Josephson effect in FeBS has been already studied by using a number of different methods [22–41]. However, most of these studies, except a few cases [25–27], deal with the so-called hybrid Josephson junction in which the junction is formed by a conventional (s-wave) superconductor and the ($s_{\pm}$ or s_{++}) FeBS. We focus here on the case of an all-FeBS coplanar Josephson junction, in which both the electrodes are FeBS materials (symmetric junction), as occurs for instance in grain boundary junctions. So far, several Josephson junctions using thin films have been fabricated [21,42–50] on bicrystal substrates (for a review on Fe-based Josephson junctions, see Ref. [51], and references therein) and thus a theoretical effort along this direction is needed.

Thus we consider a Josephson junction model in which the electrodes are two-band FeBS. To this end the junction is represented by a network of four one-dimensional branches connected to a single node point $x = 0$ (see Fig. 1), x being the coordinate along the propagation direction normal to the interface. Each superconducting branch represents the ith band on the left or the right side of the junction, while the band wave function $\Psi_i = \theta(-x)\Psi_i^{S_L}(x) + \theta(x)\Psi_i^{S_R}(x)$, in the clean limit, obeys the equation

$$\begin{bmatrix} \hat{H}_j(x) & \Delta_j(x) \\ \Delta_j^*(x) & -\hat{H}_j^*(x) \end{bmatrix} \Psi_j = E\Psi_j, \tag{1}$$

where $j \in \{\alpha,\beta\}$ is the band index, while

$$\Delta_j(x) = \Delta_j e^{i\varphi_j}\theta(-x) + \Delta_j e^{i(\varphi_j+\varphi)}\theta(x), \tag{2}$$

[$\theta(x) = 0$ for $x \leqslant 0$, $\theta(x) = 1$ for $x > 0$] are the two coexisting pair potentials. The operator $\hat{H}_j(x)$ represents the single-particle Bogoliubov–de Gennes (BdG) Hamiltonian in the two bands, which reads

$$\hat{H}_j(x) = -\frac{\hbar^2}{2m_j}\frac{\partial^2}{\partial x^2} - E_F. \tag{3}$$

In writing Eq. (2) we are neglecting the proximity effect and assuming that the inhomogeneous character of the gap in the junction is captured by choosing $\Delta_\alpha = \Delta_\beta = 0$ just at the node (short junction). The two gap values Δ_α, Δ_β, with $\Delta_\alpha < \Delta_\beta$, are assumed to be the same in the two superconductive leads. The quantity φ is the gauge invariant phase difference between the two superconductive regions; φ_α and φ_β are the internal pair potential phases. In the case of $s_{\pm}$-wave gap model, $\varphi_\beta - \varphi_\alpha = \pi$ and the two gaps have opposite sign, while in the standard two band model, with same sign gaps, $\varphi_\beta - \varphi_\alpha = 0$. The quantities m_j in Eq. (3) are the effective masses of quasiparticles in the jth superconducting branch and are material-dependent quantities. We also introduce a single-particle node potential $U(x)$ which is different from zero only for $x = 0$ and can be modeled as the usual Blonder-Tinkham-Klapwijk [52] interface potential $U(x) = U_0\delta(x)$, even though this limiting assumption is not required to develop the theory. The node potential $U(x)$ allows the modeling of a FeBS/insulator/FeBS or FeBS/normal-metal/FeBS junction in which a normal scattering at the interface reduces the transparency of the junction. The junction barrier strength can be still characterized by introducing a Blonder-Tinkham-Klapwijk dimensionless parameter $Z = mU_0/(\hbar^2 k_F)$ (m being the bare electron mass and $k_F^2 = 2mE_F/\hbar^2$) within the boundary conditions of the scattering problem. The modified boundary conditions used here [see Eqs. (8) and (9)] account for band-sensitive scattering effects and have been already introduced in Ref. [20] to describe the differential conductance of a normal-metal/FeBS junction; in the following we discuss their generalization to the Josephson junction case. The potentials $U(x)$ and $\Delta_j(x)$ are responsible for the normal scattering and the scattering of electrons into holes (Andreev scattering) at the interface, respectively. The four wave functions, $\Psi_j^{S_L}(x)$, $\Psi_j^{S_R}(x)$ ($j = \alpha,\beta$), one for each branch in the two electrodes, can be written in terms of the eigenstates of the local Hamiltonians as

$$\Psi_j^{S_L}(x) = \begin{bmatrix} u_j^L(x) \\ v_j^L(x) \end{bmatrix} = a_j \begin{pmatrix} v_j \\ u_j e^{-i\varphi_j} \end{pmatrix} e^{ip_h^j x} + b_j \begin{pmatrix} u_j \\ v_j e^{-i\varphi_j} \end{pmatrix} e^{-ip_e^j x}, \tag{4}$$

for $x < 0$ or

$$\Psi_j^{S_R}(x) = \begin{bmatrix} u_j^R(x) \\ v_j^R(x) \end{bmatrix} = c_j \begin{pmatrix} u_j \\ v_j e^{-i(\varphi_j+\varphi)} \end{pmatrix} e^{ip_e^j x} + d_j \begin{pmatrix} v_j \\ u_j e^{-i(\varphi_j+\varphi)} \end{pmatrix} e^{-ip_h^j x}, \tag{5}$$

for $x > 0$. Here u_α, v_α and u_β, v_β are the Bogoliubov coefficients for the first and second bands, respectively:

$$u_j = \left[\frac{1}{2}\left(1 + i\frac{\Omega_j}{E}\right)\right]^{1/2}, \quad v_j = \left[\frac{1}{2}\left(1 - i\frac{\Omega_j}{E}\right)\right]^{1/2} \tag{6}$$

with $\Omega_j = \sqrt{\Delta_j(T)^2 - E^2}$, $j \in \{\alpha,\beta\}$, while T represents the temperature of the thermal bath. The wave vectors of the two bands,

$$p_{e,h}^{j} = \sqrt{r_j^2 k_F^2 \pm 2 i m_j \Omega_j/\hbar^2},$$

are well approximated by the expressions

$$\begin{aligned} p_{e,h}^{\alpha} &\simeq r_\alpha k_F\left(1 \pm i\chi\sqrt{1 - E^2/{\Delta_\alpha}^2}\right), \\ p_{e,h}^{\beta} &\simeq r_\beta k_F\left(1 \pm i\chi\sqrt{{\Delta_\beta}^2/{\Delta_\alpha}^2 - E^2/{\Delta_\alpha}^2}\right), \end{aligned} \tag{7}$$

which are valid under the assumption $E_F \gg \Delta_\beta$, while the different signs $+,-$ refer to electronlike or holelike excitations, respectively. The coefficient $r_j^2 = m_j/m$ represents the effective mass of the jth band measured in units of the bare electron mass m. In writing Eq. (7) we have introduced the dimensionless factor $\chi = \Delta_\alpha(T)/2E_F$ or $\chi = \Delta_\alpha(T)/(k_F v_F \hbar)$, which represents the ratio between the Fermi wavelength k_F^{-1} and the coherence length $\xi(T) \sim \hbar v_F/\Delta_\alpha(T)$. Its zero-temperature value, χ_0, can be also defined as $\chi_0 = \Delta_\alpha(0)/(2E_F)$. Since we are interested in localized subgap states, in Eq. (7) we assume $E < \Delta_\alpha(0)$, ensuring that the wave functions $\Psi_j^{S_L}(x)$, $\Psi_j^{S_R}(x)$ $(j = \alpha,\beta)$ decay exponentially for $|x| \to \infty$.

The quasiparticle wave functions obey the generalized matching quantum waveguide conditions [20]

$$\begin{aligned} &\Psi_\alpha^{S_R}(0) = s_\alpha \Psi_\alpha^{S_L}(0), \quad \Psi_\beta^{S_R}(0) = s_\beta \Psi_\alpha^{S_L}(0), \\ &\Psi_\beta^{S_L}(0) = s \Psi_\alpha^{S_L}(0), \end{aligned} \tag{8}$$

$$\begin{aligned} &\frac{\partial}{\partial x}\left[s_\alpha \frac{1}{r_\alpha^2}\Psi_\alpha^{S_R} + s_\beta \frac{1}{r_\beta^2}\Psi_\beta^{S_R}\right]_{x=0} - \frac{\partial}{\partial x}\left[\frac{1}{r_\alpha^2}\Psi_\alpha^{S_L} + s\frac{1}{r_\beta^2}\Psi_\beta^{S_L}\right]_{x=0} \\ &= 2k_F Z \Psi_\alpha^{S_L}(0). \end{aligned} \tag{9}$$

Equations (8) and (9) guarantee the conservation of the charge current at the node $x = 0$ (quantum Kirchhoff's law) and generalize the waveguide boundary conditions given in Ref. [20] to the Josephson junction case. The three parameters s_α, s_β, s characterize the interface and make the scattering processes and the current flow band-sensitive. Indeed, the overlap between the wave functions on different sides of the junction may favor scattering events towards a specific band, α or β. The existence of these "band coupling parameters" implies that a discontinuity of the wave functions may occur at the node $(x = 0)$ when at least one of the coupling parameters s_α, s_β, s is different from 1. The meaning of this discontinuity has been discussed in Ref. [20] in connection with the theory of PCARS in multiband superconductors. The physical meaning of the overlap parameters s_α, s_β, s can be easily understood by observing that setting, for instance, $s_\alpha = 0$ implies $\Psi_\alpha^{S_R}(0) = 0$. Thus the wave function $\Psi_\alpha^{S_R}(x)$ presents a vanishing overlap at the interface with the remaining branch wave functions. As a consequence, in this case, the band α on the right side of the junction is excluded from the transport. The latter point can be further clarified by looking at the prefactor of the first term of Eq. (9), namely $s_\alpha(m_\alpha/m)^{-1}$, which governs the particle flow through the α band on the right side of the junction. Lowering s_α has the same effect of increasing m_α, causing a lowering of the particle flux through the considered band. In the equal coupling case $(s_\alpha = s_\beta = s = 1)$ the partitioning of the current among different network branches is entirely governed by the bulk mass ratios r_j and only weakly affected by the interface scattering potential strength Z. Thus the parameters s_α, s_β, s can be properly interpreted as overlap or coupling factors which define the fraction of current flowing through a specific band.

Equations (8) and (9) provide a linear system of equations for the eight unknown coefficients a_j, b_j, c_j, d_j $(j \in \{\alpha,\beta\})$ appearing in the wave functions (see Appendix A). The bound state spectrum can be determined by imposing the condition that this homogeneous system of equations has a nontrivial solution. Within the Andreev approximation, i.e., $p_e^\alpha \simeq p_h^\alpha \simeq r_\alpha k_F$ and $p_e^\beta \simeq p_h^\beta \simeq r_\beta k_F$, this critical condition is written as

$$\begin{aligned} &-\frac{s_\beta^2(\epsilon^2-\gamma^2)\left[1-\epsilon^2-2s_\alpha^2\epsilon^2 - s_\alpha^4(\epsilon^2-1) + 2s_\alpha^2\cos\varphi\right]}{r_\alpha^2} + \frac{s^2(\epsilon^2-1)\left[2ss_\beta^2\epsilon^2 + \left(s^2+s_\beta^4\right)(\epsilon^2-\gamma^2) - 2ss_\beta^2\gamma^2\cos\varphi\right]}{r_\beta^2} \\ &+ \frac{2ss_\beta\sqrt{\epsilon^2-1}\sqrt{\epsilon^2-\gamma^2}\left(s\left[\left(1+s_\alpha^2\right)\epsilon^2 - e^{i\delta}\gamma\right] + s_\beta^2\left[\left(1+s_\alpha^2\right)\epsilon^2 - e^{i\delta}s_\alpha^2\gamma\right] - e^{i\delta}\left(ss_\alpha^2 + s_\beta^2\right)\gamma\cos\varphi\right)}{r_\alpha r_\beta} \\ &+ 4s_\beta^2 Z^2(\epsilon^2-1)(\epsilon^2-\gamma^2) = 0, \end{aligned} \tag{10}$$

where $\delta = \varphi_\beta - \varphi_\alpha$, $\gamma = \Delta_\beta/\Delta_\alpha$, and $\epsilon = E/\Delta_\alpha(T)$. Choosing $\delta = 0$ or $\delta = \pi$ reflects the internal pairing symmetry s_{++} or $s_{\pm}$, respectively. Two sets of energy levels $E^+(\varphi)$ and $E^-(\varphi)$ are found in solving Eq. (10), which correspond to electronlike and holelike quasiparticles, respectively. One finds that the Andreev bound states never appear beyond Δ_α. When $s_\alpha = s_\beta = s = 1$, in the two limits $r_\alpha \to \infty$ or $r_\beta \to \infty$ (exclusion of the α or β band respectively), Eq. (10) provides the well known s-wave result $E = E_B = \Delta_j\sqrt{[\cos^2(\varphi/2) + Z_j^2]/(1+Z_j^2)}$, with $Z_j = r_j Z$ [53], j being α or β [see Fig. 2(c)].

In Fig. 2 we show Andreev bound states spectra computed using Eq. (10). Once the mass ratios r_j have been fixed, different Josephson couplings can be obtained depending on the kind of the order parameter symmetry and on the choice of the overlap factors. To better explain this point, we present different curves obtained by letting the parameter s_α vary in the range (1,0.3) in steps of -0.1, while $s_\beta = s = 1$. This choice of the overlap factors corresponds to progressively weakening the coupling of the band $\Psi_\alpha^{S_R}$ from the remaining bands. Panels (a) and (b) $(r_\alpha = 1.8, r_\beta = 1)$ show a generalized lowering of the levels toward the zero-energy state in the case of $s_\pm$ symmetry [panel (a)], which is absent in the case of

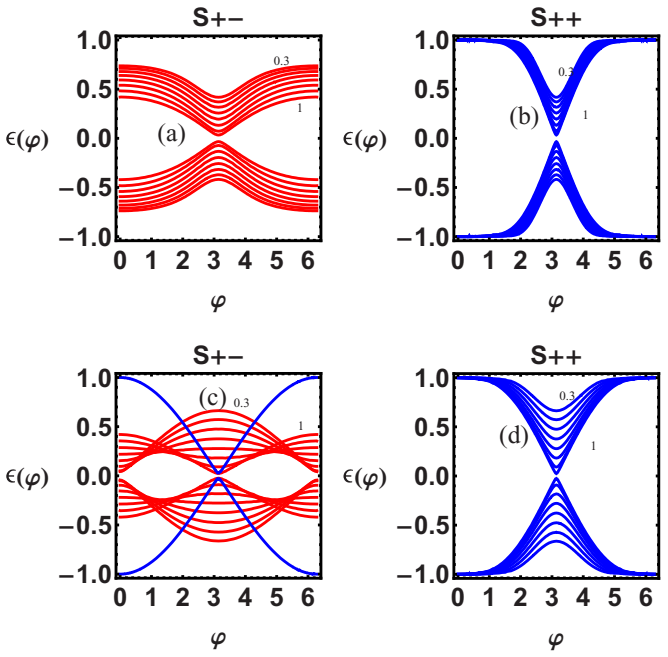

FIG. 2. (Color online) Bound states energy levels $E^{+}(\varphi)$ and $E^{-}(\varphi)$ [normalized to $\Delta_\alpha(T)$] calculated through Eq. (10). Panels (a) and (c): $s_\pm$ symmetry. Panels (b) and (d): s_{++} symmetry. Z and γ have been fixed to $Z = 0.03$ and $\gamma = 3$, the various curves are obtained by letting parameter s_α to vary in the range (0.3,1) in steps of 0.1, while $s_\beta = s = 1$. Panels (a) and (b): $r_\alpha = 1.8$, $r_\beta = 1$. Panels (c) and (d): $r_\alpha = 1$, $r_\beta = 1.8$; the darker curve (blue line in color version) in panel (c) is the Andreev level of a conventional s-wave junction with $r_j Z = 0.03$.

s_{++} symmetry [panel (b)] and represents the main difference between the two symmetries in this case. A further difference is illustrated in panels (c) and (d) ($r_\alpha = 1$, $r_\beta = 1.8$). In the case of $s_\pm$ symmetry [panel (c)] the energy levels undergo a gradual concavity change as the parameter s_α is decreased. This concavity change is responsible for a π-shift in the current-phase relation, which is not observed in the s_{++} case [Fig. 2(d)]. Thus, as also observed elsewhere [25], a 0–π transition may be a distinctive signature of the $s_\pm$ symmetry. This point will be further explained in Sec. IV, where the current-phase relations and the temperature dependence of the maximum Josephson current will be presented.

III. JOSEPHSON CURRENT

The Josephson current flowing through the junction could be directly computed from the Andreev bound states according to the formula [54]

$$I_J(\varphi) \approx -\frac{2e}{\hbar}\frac{dE^{+}(\varphi)}{d\varphi}\tanh\left[\frac{E^{+}(\varphi)}{2k_BT}\right]. \tag{11}$$

Due to the special character of the bound state of a multiband junction, in the following we will characterize the Josephson current by using a field theory formalism in second quantization. We verified that the latter procedure provides results consistent with those obtained using Eq. (11).

The Cooper-pair charge flow $\bar{J}_{ch}$ through the junction can be computed as a quantum-statistical average of the current density operator according to the expression $\bar{J}_{ch} = \sum_{j,\sigma}\langle\hat{\psi}^{\dagger}_{j\sigma}\check{\mathcal{J}}_j\hat{\psi}_{j\sigma}\rangle$, where $\check{\mathcal{J}}_j = \frac{i\hbar|e|}{2m_j}(\overrightarrow{\partial}_x - \overleftarrow{\partial}_x)$ represents the first-quantization band operator [55]. The second quantized fields $\hat{\psi}_{j\sigma}$ ($\hat{\psi}^{\dagger}_{j\sigma}$) represent the annihilation (creation) operators of a spin σ electron in the jth band and obey a fermionic algebra. These fields provide an appropriate basis in the absence of superconducting correlations. However, when the superconductivity is established, $\hat{\psi}_{j\sigma}$ are not eigenfields of the problem and, for this reason, the Nambu representation can be conveniently used: $\Psi(x) = \sum_{j\in\{\alpha,\beta\}}|j\rangle\otimes(\hat{\psi}_{j\uparrow},\hat{\psi}^{\dagger}_{j\downarrow})^t$. The Nambu field $\Psi(x)$ is a nonlocal quantity describing particle-hole excitations in different network branches and can be expanded in eigenfields of the Hamiltonian problem on the network. Limiting the expansion to the eigenfields $\hat{\gamma}_\sigma$ describing the low-energy (sub-gap) states with energy $\pm E_B \in [-\Delta_\alpha,\Delta_\alpha]$, we get

$$\Psi(x) \approx \hat{\gamma}_\uparrow e^{-iE_Bt/\hbar}\psi_B(x) + \hat{\gamma}^{\dagger}_\downarrow e^{iE_Bt/\hbar}\tilde{\psi}_B(x), \tag{12}$$

where $\psi_B(x) = \theta(-x)\psi^{(L)}_B(x) + \theta(x)\psi^{(R)}_B(x)$ is the wave function of the electronlike bound state having energy eigenvalue $E_B > 0$, while $\tilde{\psi}_B(x) = [\sum_j |j\rangle\langle j|\otimes i\hat{\sigma}_y\mathcal{C}]\psi_B(x)$ represents its time-reversed state associated with a holelike state with energy $-E_B$. The electronlike bound state is localized at the interface and extends over all the waveguide branches. Thus eigenstates of the local branch Hamiltonians can be used to expand $\psi_B(x)$, using the following decomposition:

$$\psi^{(\nu)}_B(x) = \sum_{j\in\{\alpha,\beta\}}|j\rangle\otimes\begin{bmatrix}u^{\nu}_j(x)\\ v^{\nu}_j(x)\end{bmatrix}, \tag{13}$$

with $\nu\in[L,R]$ an index identifying the left ($x<0$) or right ($x>0$) side of the junction. Once $\Psi(x)$ has been expanded in eigenfields $\hat{\gamma}_\sigma$ it is possible to recognize the fermionic fields $\hat{\psi}_{j\uparrow}$ in the expression

$$\hat{\psi}_{j\uparrow} \approx \hat{\gamma}_\uparrow e^{-iE_Bt/\hbar}u_j(x) - \hat{\gamma}^{\dagger}_\downarrow e^{iE_Bt/\hbar}v_j(x)^*, \tag{14}$$

with $u_j(x) = \theta(-x)u^L_j(x) + \theta(x)u^R_j(x)$ and analogously for $v_j(x)$. Substituting Eq. (14) in the expression for $\bar{J}_{ch}$, in the absence of spin-sensitive potentials [56], we obtain ($x>0$)

$$\bar{J}_{ch} = \frac{-2|e|\hbar}{m}\sum_j r_j^{-2}\big\{\mathrm{Im}\big[u^R_j(x)^*\partial_x u^R_j(x)\big]f(E_B) + \mathrm{Im}\big[v^R_j(x)\partial_x v^R_j(x)^*\big][1-f(E_B)]\big\}, \tag{15}$$

where we explicitly used the thermal equilibrium averages $\langle\hat{\gamma}^{\dagger}_\sigma\hat{\gamma}_\sigma\rangle = f(E_B)$ and $\langle\hat{\gamma}_\sigma\hat{\gamma}^{\dagger}_\sigma\rangle = 1-f(E_B)$. Due to current conservation we have the freedom to evaluate the current in $x = 0^+$, and thus starting from Eq. (15) we get ($e=-|e|$) [57]

$$\bar{J}_{ch} = -2ev_F\sum_j\frac{u_jv_j}{r_j}(|c_j|^2-|d_j|^2)\tanh\left[\frac{E_B}{2k_BT}\right], \tag{16}$$

where the coefficients $c_j(\varphi)$ and $d_j(\varphi)$ are calculated at the energy $E_B = \epsilon_B(\varphi)\Delta_\alpha(T)$, while $\epsilon_B(\varphi)$ is solution of Eq. (10). It is worth mentioning here that the Fermi velocity in the ith band is given by $v^{(i)}_F = v_F/r_i$, while the quantity $v_F = \hbar k_F/m$ is just used as the velocity unit. Equation (16) is one of the main results of this work and generalizes the expression found in Ref. [58] to the multiband case.

Equation (16), complemented by the coefficients c_j and d_j derived following the procedure sketched in Appendix A, allows us to obtain the current-phase relation of the junction at all temperatures. The Josephson current [Eq. (16)] is parametrized by the barrier strength Z and the overlap parameters s_α,s_β,s. These parameters characterize the multiband superconductor junction and can be determined by fitting the current phase relation as well as the temperature dependence of the critical current of the junction. In deriving the scattering coefficients a_j, b_j, c_j, d_j ($j \in \{\alpha,\beta\}$), Eqs. (8) and (9) have to be complemented by the normalization condition, $\int_{-\infty}^{\infty} dx \psi_B(x)^\dagger \psi_B(x) = 1$, of the bound state wave function $\psi_B(x)$: $\sum_{j=\alpha,\beta} \int_{-\infty}^{0} [|u_j^L(x)|^2 + |v_j^L(x)|^2]dx + \sum_{j=\alpha,\beta} \int_0^{+\infty} [|u_j^R(x)|^2 + |v_j^R(x)|^2]dx = 1$. The normalization condition can be satisfied only by considering an imaginary part in the expressions of the quasiparticle momenta p_e^j and p_h^j. This accounts for the localized nature of the bound state, whose wave function contains decaying exponentials of the type $\sim \exp[\pm\chi r_\alpha k_F \sqrt{1-(E_B/\Delta_\alpha)^2}x]$ and $\sim \exp[\pm\chi r_\beta k_F \sqrt{\gamma^2-(E_B/\Delta_\alpha)^2}x]$, the decay length being comparable with the coherence length $\xi(T) \sim \hbar v_F/\Delta_\alpha(T)$. Due to the different decay lengths characterizing the bound state wave function, $|E_B|$ cannot exceed Δ_α. Indeed, assuming $E_B > \Delta_\alpha$, the quantum state is no longer localized and its wave function $\psi_B(x)$ is not normalizable. The above arguments explains why the bound state energy E_B cannot exceed the minimum value among the superconducting gaps describing the multiband junction. This latter aspect suggests that the performances of a multiband Josephson junction can be strongly affected by disorder effects and inhomogeneities.

IV. NUMERICAL RESULTS

In this section we provide specific examples of the current-phase relation derived through Eq. (16). We assume that the temperature dependence of both gaps Δ_j ($j = \alpha,\beta$) is given by $\Delta_j(T) = \Delta_j(0)\tanh(1.74\sqrt{T_c/T-1})$, where T_c is the critical temperature of the superconducting transition. We also assume the validity of the BCS ratio $\Delta_\alpha(0)/k_B T_c = 1.76$ between the critical temperature and the zero-temperature pair potential. Under these assumptions, the parameter $\gamma = \Delta_\beta/\Delta_\alpha$ does not depend on the temperature. Note that the quantity χ_0 has been assigned the value 0.01 in the calculations but that the results do not depend on the specific value of χ_0, provided that $\chi_0 \ll 1$.

In Fig. 3 we present the current-phase relation of two junction configurations whose bound states energy has been shown in Fig. 2. In particular, in panels (a) and (b), we report the current-phase relations computed for the $s_\pm$ and the s_{++} symmetry, respectively, setting the model parameters as follows: $Z = 0.03$, $\gamma = 3$, $r_1 = 1.8$, $r_2 = 1$. The different curves are obtained by letting the parameter s_α vary in the range (0.3,1) in steps of 0.1, while $s_\beta = s = 1$. One notices, besides the weak dependence of the various curves on s_α in both panels (a) and (b) of Fig. 3, a suppression of the Josephson current by a factor $3 \sim \gamma$ in the $s_\pm$ symmetry

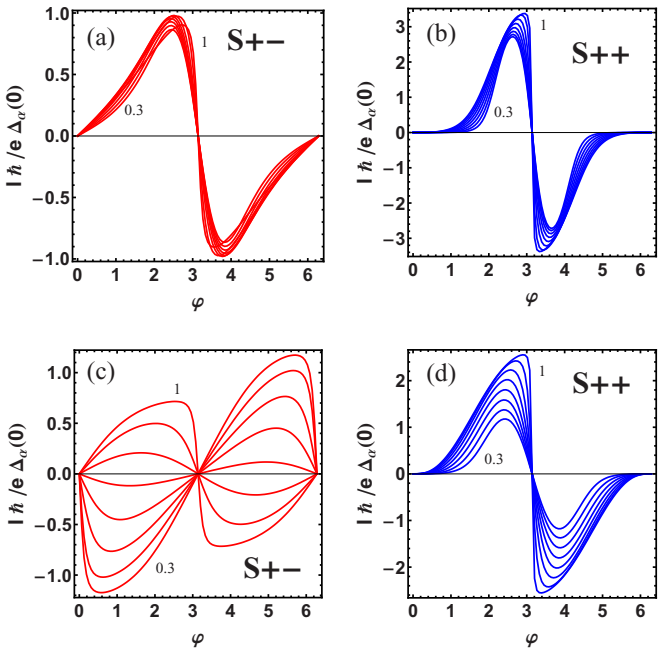

FIG. 3. (Color online) Current-phase relations at $T = 0.001T_c$. Panels (a) and (c): $s_\pm$ symmetry. Panels (b) and (d): s_{++} symmetry. Parameters are the same as those of the corresponding panels in Fig. 2; (a) and (b): $Z = 0.03$, $\gamma = 3$, $r_1 = 1.8$, $r_2 = 1$; (c) and (d): $Z = 0.03$, $\gamma = 3$, $r_1 = 1$, $r_2 = 1.8$. The value of χ_0 has been set to $\chi_0 = 0.01$. The various curves are obtained by letting parameter s_α vary in the range (0.3,1) in steps of 0.1, while $s_\beta = s = 1$.

[panel (a)] compared to the s_{++} case [panel (b)]. The latter phenomenon originates from the destructive interference effects of quasiparticles experiencing two opposite gap signs. The destructive interference lowers the Andreev reflection probability such that, in perfectly symmetric junctions (i.e., $r_\alpha = r_\beta$, $s_\alpha = s_\beta = s = 1$), the current would exactly vanish. Thus s_{++} Josephson junctions exhibit greater critical current values [$I_c(T \to 0) \sim e\Delta_\beta/\hbar$] compared to those expected for the $s_\pm$ case [$I_c(T \to 0) \sim e\Delta_\alpha/\hbar$]. On the other hand, the peculiar functional form of the current-phase relations of the s_{++} symmetry [panel (b)] indicates a certain fragility of this junction against bias current fluctuations. Indeed, a small bias fluctuation (less than few percent of the critical current) can cause, at low bias, a relevant phase fluctuation. This stochastic phase jump may represent a relevant source of voltage fluctuation across the junction which can also drive the system towards an Ohmic regime.

Figures 3(c) and 3(d) are obtained by setting $r_\alpha = 1.8$ and $r_\beta = 1$, while maintaining the remaining parameters at the same values fixed in the upper panels of Fig. 3. Again, a suppression of the current amplitude by a factor 3 between the $s_\pm$ symmetry and s_{++} symmetry appears [compare the curves corresponding to $s_\alpha = 1$ in panels (c) and (d) respectively]. Moreover, the sign change of the pair potential in the $s_\pm$ symmetry is made evident by lowering s_α ($s_\alpha = 1, 0.9, \ldots, 0.3$); this lowering determines the gradual phase shift and the formation of a π state in the curves of panel (c), while curves in panel (d) do not present this

phenomenology. A π-state Josephson junction (π junction) exhibits negative critical current and a minimum of the free energy $F(\varphi) = \Phi_0/2\pi \int_0^{\varphi} d\theta\, I(\theta)$ located at $\varphi = \pi$ rather than $\varphi = 0$. The existence of π-shifted junctions can be experimentally proved employing superconducting quantum interference device (SQUID) measurements [15,59–61].

The study of the CPR may provide important information about a Josephson junction's parameters [62]. The determination of the parameters Z, s_α, s_β, s, i.e., the Josephson spectroscopy of the multiband superconductor, can be achieved through a current-phase relation measurement and a direct comparison with Eq. (16). Most of the methods employed for the experimental investigation of the current-phase relation are re-elaborations of the rf technique proposed in 1967 by Silver and Zimmerman [63]. An important point is that the CPR can be extracted from experimental data without any fitting parameters [64]. The method has been refined in the years by many researchers, in particular Il'ichev and coworkers, who measured the CPR of YBCO junctions [14,65,66] and also demonstrated that current-phase relation measurements are much less sensitive to thermal fluctuations than other junctions' properties measurements [67]. The CPR measurement technique has been recently [68] applied in topological insulator-superconductor systems where it may potentially reveal the surface ballistic nature of an induced superconducting state or even the presence of Majorana fermions. In the case of iron-pnictides the present theory predicts strongly characterized behaviors of the CPRs such that this type of measurement may be pivotal in helping to discriminate between $s_\pm$ and s_{++} symmetries or also in determining the degree of coupling between various bands. In iron based superconductors the superconducting order parameters $\Delta_\alpha, \Delta_\beta$ coexist with a magnetic order parameter (spin density wave) [26,69], so that experiments should be performed in a regime where the effects of a spin density wave order can be neglected.

Besides the CPR experiments, the measurement of the temperature dependence of the junction critical current $I_c(T)$ represents an important independent tool useful for identifying the nature of the superconducting pairing [70–72]. Thus, in order to compare our results with the experimental findings, we have derived the temperature dependence of the maximum Josephson current (critical current). Figure 4 shows the temperature dependence of the critical current calculated for the $s_\pm$ [(a) and (c)] and s_{++} symmetries [(b) and (d)] by setting the model parameters as in Figs. 2 and 3. Negative critical current values, like those presented in panel (c), indicate a π-shifted Josephson junction. A common feature of all the panels in Fig. 4 is the violation of the Ambegaokar-Baratoff relation, which is usually reported in multiband S/I/S Josephson junctions [73]. The extent of such a violation depends on the junction parameters and is more pronounced for the $s_\pm$ symmetry [see panels (a) and (c)], where the critical current vs temperature curves develop a peculiar positive curvature. Panels (b) and (d) are described by a deformed Ambegaokar-Baratoff relation and suggest that a π junction cannot be observed for the s_{++} symmetry. In this respect we observe that the 0–π transition reported in the present work [see Figs. 3(c) and 4(c)] is the result of a different mechanism

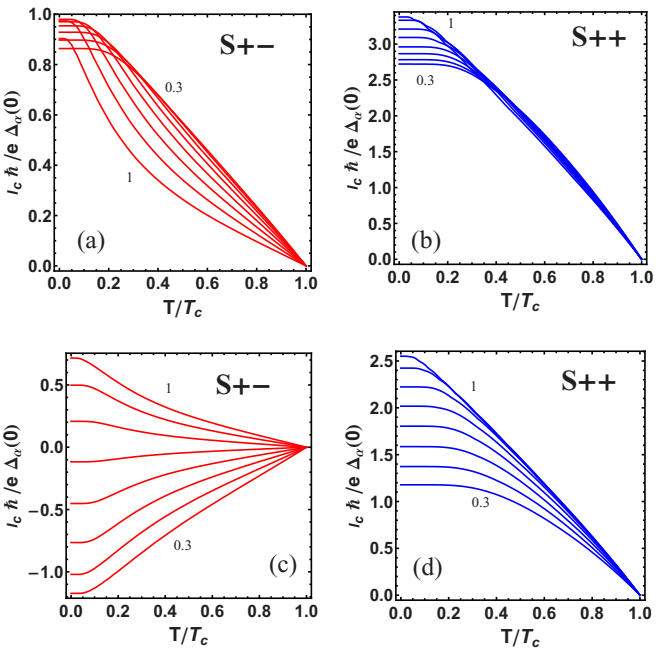

FIG. 4. (Color online) Josephson critical current as a function of the reduced temperature T/T_c. Panels (a) and (c): $s_\pm$ symmetry. Panels (b) and (d): s_{++} symmetry. Parameters are the same as those of the corresponding panels in Fig. 2: $Z = 0.01$, $\gamma = 3$. The value of χ_0 has been set to $\chi_0 = 0.01$. (a) and (b): $r_1 = 1.8$, $r_2 = 1$. (c) and (d): $r_1 = 1$, $r_2 = 1.8$. The critical current is in units of $e\Delta_\alpha(0)/\hbar$. The various curves are obtained by letting parameter s_α vary in the range (0.3,1) in steps of 0.1, while $s_\beta = s = 1$.

compared to the one described in Ref. [25]. There the transition originates from the competition of two Andreev bound states carrying opposite current. As the temperature is lowered, the state with higher energy eigenvalue is progressively excluded from the transport and a sign reversal of the critical current is observed. Here we predict the presence of a single electronlike bound state and thus a temperature activated 0–π transition cannot be observed as an intrinsic effect. However, direct tunneling ($\alpha \to \alpha$ or $\beta \to \beta$) and crossed tunneling ($\alpha \to \beta$ or $\beta \to \alpha$) effects provide a supercurrent contribution with opposite sign and thus, depending on the relative strength of these contributions, a π junction can be formed only by assuming the $s_\pm$ symmetry. The relative strength of the direct and crossed tunneling contributions is controlled in the model by the overlap parameters s_α, s_β, and s which are characteristic of the interface. According to these arguments, a 0–π transition can occur by varying at least one overlap parameter. This can be done in different ways: (i) changing the temperature can induce a lattice deformation at the interface which is relevant in determining the overlap parameters; (ii) experiments performed under controllable pressure or strain allow one to control lattice distortion and thus the overlap parameters. Both methods (i) and (ii) can be used to induce the 0–π transition in multiband Josephson junctions. The mechanism of formation of a π junction described above can

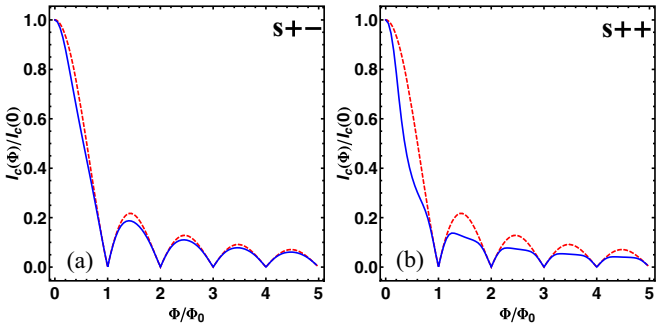

FIG. 5. (Color online) Normalized critical current $I_c(\Phi)/I_c(0)$ as a function of the applied magnetic flux Φ/Φ_0 computed for the $s_\pm$ [panel (a)] and s_{++} symmetries [panel (b)]. Parameters are the same as those of the corresponding panels in Fig. 3: $Z = 0.03$, $\gamma = 3$, $r_1 = 1.8, r_2 = 1, s_\alpha = s_\beta = s = 1, \chi_0 = 0.01$, and $T = 0.001T_c$. The dashed curve in each panel represents the Fraunhofer pattern for comparison.

be also recovered in the framework of a semiclassical theory of the $s_\pm/I/s_\pm$ Josephson junction as developed in Ref. [74], or within the framework of the tunneling Hamiltonian method as reported in Ref. [26] [see Eq. (5)].

However, as clearly evidenced in Figs. 3(a) and 3(b), the 0–π transition is strongly affected by the band's effective mass and can remain unobserved also for an $s_\pm$ junction. Under this condition, the magnetic response of the system (see Appendix B for details) provides an indirect probe of the harmonic content of the current-phase relation and can help in discriminating the pairing symmetry of the junction. In particular, the zero-field critical current $I_c(0)$ of the s_{++} case [see Fig. 3(b)] is greater than the corresponding value obtained for the $s_\pm$ case [see Fig. 3(a)]. As a consequence, one expects that the harmonic content of the current-phase relation of the s_{++} case strongly affects the low-field magnetic diffraction pattern of the junction. On the other hand, for the $s_\pm$ case, the high harmonic contribution is expected to be less important due to the lower value of zero-field critical current. The above arguments are confirmed by Fig. 5 where the normalized critical current $I_c(\Phi)/I_c(0)$ is studied as a function of the applied magnetic flux Φ/Φ_0 (normalized to the flux quantum Φ_0) for the $s_\pm$ [panel (a)] and s_{++} [panel (b)] symmetries, while the model parameters are fixed as done for the corresponding panels in Fig. 3. Interestingly, the s_{++} Josephson junction evidences a critical current halving already for flux values of $\sim 0.4\Phi_0$, while the critical current of the $s_\pm$ case is less sensitive to magnetic field effects.

V. CONCLUSIONS

We have formulated a minimal model of the dc Josephson effect for multiband superconductors based on the quantum waveguide approach. The method is based on the analogy between multiband superconductors and multibranch networks recently suggested in Ref. [18]. Accordingly, the subgap bound states wave functions (electron- and holelike), relevant in describing the quantum transport within the short junction limit, are decomposed using the eigenstates of local branch Hamiltonians, and the coefficients of such a decomposition are found by imposing generalized boundary conditions on the wave functions. The boundary conditions are a direct generalization of those used in Ref. [20] and incorporate a local scattering potential at the interface (Z parameter) and band overlap factors s_α, s_β, and s which define the weight of each band in the quasiparticles transport. This provides an effective parametrization of the interface effects, allowing us to describe Josephson junctions ranging from the metallic ($Z \ll 1$) to the tunnel limit ($Z \gg 1$). The bulk properties of the superconducting bands are introduced using different effective masses (r_j parameters) which can be determined by complementary experiments. We have solved the scattering problem and we have determined the Andreev bound states spectrum and the normalized eigenfunctions. The Josephson current flowing through the junction has been computed using a second quantization approach which correctly reproduces results obtained using the phase derivative of the Andreev bound states spectrum formula. The second quantization method used in the derivation of the Josephson current generalizes the result presented in Ref. [58] for a single-band superconductor to the multiband case and represents one of the main results of this work. To provide a specific and relevant application of the theory, we have focused our treatment on FeBS-FeBS tunnel junctions. In particular, we have derived the current-phase relations and the critical currents of symmetric FeBS junctions modeled as superconducting systems with two relevant bands. We have analyzed s_{++} and $s_\pm$ symmetries of the FeBS and we have shown that a π junction can be observed only for $s_\pm$ symmetry and under appropriate interface conditions, which are carefully discussed in the text. Further peculiar aspects of FeBS-FeBS tunnel junctions are also discussed. The above findings are relevant for the Josephson effect theory in multiband systems and can contribute to the current debate about the order parameter symmetry of iron-based materials.

ACKNOWLEDGMENTS

This work has been partially supported by the financial contribution of EU NMP.2011.2.2-6 IRONSEA Project No. 283141. R.C. acknowledges the project FIRB-2012-HybridNanoDev (Grant No. RBFR1236VV). The authors gratefully acknowledge Roberto De Luca for useful discussions on the topic of this work.

APPENDIX A: DETERMINATION OF THE SCATTERING COEFFICIENTS

The matching conditions Eqs. (8) and (9) provide the linear homogeneous system $\mathbf{M} \cdot \mathbf{X} = 0$, where $\mathbf{X} = (a_\alpha, \ldots, d_\alpha, a_\beta, \ldots, d_\beta)^t$ and $\mathbf{M}$ is the following

matrix:

$$\begin{pmatrix}
s_\alpha v_\alpha & s_\alpha u_\alpha & -u_\alpha & -v_\alpha & 0 & 0 & 0 & 0 \\
s_\alpha u_\alpha & s_\alpha v_\alpha & -e^{-i\varphi} v_\alpha & -e^{-i\varphi} u_\alpha & 0 & 0 & 0 & 0 \\
0 & 0 & 0 & 0 & s_\beta v_\beta & s_\beta u_\beta & -u_\beta & -v_\beta \\
0 & 0 & 0 & 0 & e^{-i\delta} s_\beta u_\beta & e^{-i\delta} s_\beta v_\beta & -e^{-i(\delta+\varphi)} v_\beta & -e^{-i(\delta+\varphi)} u_\beta \\
s v_\alpha & s u_\alpha & 0 & 0 & 0 & 0 & -u_\beta & -v_\beta \\
s u_\alpha & s v_\alpha & 0 & 0 & 0 & 0 & -e^{-i(\delta+\varphi)} v_\beta & -e^{-i(\delta+\varphi)} u_\beta \\
-\frac{v_\alpha(i+2r_\alpha Z)}{r_\alpha} & \frac{u_\alpha(i-2r_\alpha Z)}{r_\alpha} & \frac{i s_\alpha u_\alpha}{r_\alpha} & -\frac{i s_\alpha v_\alpha}{r_\alpha} & -\frac{i s v_\beta}{r_\beta} & \frac{i s u_\beta}{r_\beta} & \frac{i s_\beta u_\beta}{r_\beta} & -\frac{i s_\beta v_\beta}{r_\beta} \\
-\frac{u_\alpha(i+2r_\alpha Z)}{r_\alpha} & \frac{v_\alpha(i-2r_\alpha Z)}{r_\alpha} & \frac{i e^{-i\varphi} s_\alpha v_\alpha}{r_\alpha} & -\frac{i e^{-i\varphi} s_\alpha u_\alpha}{r_\alpha} & -\frac{i e^{-i\delta} s u_\beta}{r_\beta} & \frac{i e^{-i\delta} s v_\beta}{r_\beta} & \frac{i e^{-i(\delta+\varphi)} s_\beta v_\beta}{r_\beta} & -\frac{i e^{-i(\delta+\varphi)} s_\beta u_\beta}{r_\beta}
\end{pmatrix}.$$

The homogeneous system admits a nontrivial solution provided that the condition $\det(\mathbf{M}) = 0$ [Eq. (10) of the main text] is fulfilled. Since $\mathbf{M}$ is not a maximal rank matrix, the normalization condition of the bound state wave function provides a further condition to determine the coefficients vector $\mathbf{X}$.

APPENDIX B: MAGNETIC FIELD DEPENDENCE OF THE CRITICAL CURRENT

We describe the response of a Josephson junction under the application of a sufficiently weak external magnetic field $\vec{H} = H\hat{z}$ parallel to the z axis. We explicitly assume the small junction limit in which the transverse dimension L of the junction (parallel to the y axis) is comparable to or smaller than the Josephson penetration length λ_j ($L \lesssim \lambda_j$) [75]. The junction region, located at $x = 0$, presents a reduced pairing potential and thus experiences the maximum magnetic field value, while inside the electrodes the polarizing effect of the field is effectively screened by supercurrents. Due to this, the spatial dependence of the magnetic field is given by $\vec{H} = H\hat{z}\exp(-|x|/\lambda)$. Since we are interested in the bulk effect of $\vec{H}$, observing that $\int_{-\infty}^{\infty} \vec{H}\cdot\hat{z}\,dx = 2\lambda H$, we can approximate the spatial dependence of the field according to the expression $\vec{H} = \hat{z}\frac{\Phi}{L}\delta(x)$, where we introduced the magnetic flux $\Phi = 2\lambda L H$ induced by the external field and the Dirac delta function $\delta(x)$. The magnetic field $\vec{H} = \vec{\nabla}\times\vec{A}$ can be expressed in terms of the vector potential $\vec{A} = (-\frac{\Phi y}{L}\delta(x),0,0)$ which is not affected by self-fields in the considered limit. Assuming that the Zeeman term is effectively screened in the bulk of the electrodes, the presence of $\vec{H}$ affects the BdG branch Hamiltonian $H_{BdG}^{(j)}$ [Eq. (1)] only through the substitution $\hat{p}_x \to \hat{p}_x - eA_x$. The vector potential A_x can be gauged away by means of the unitary transformation

$$U = \exp\left(i\pi\frac{\Phi}{\Phi_0}\frac{y}{L}\theta(x)\hat{\sigma}_z\right), \tag{B1}$$

with $\hat{\sigma}_z$ a Pauli matrix acting on the particle-hole space and $\Phi_0 = h/(2|e|)$ the elementary flux quantum. The transformed branch Hamiltonian $\widetilde{H}_{BdG}^{(j)} = U^\dagger H_{BdG}^{(j)} U$ under the action of U can be obtained with the following substitutions:

$$\begin{aligned}
U_{11}^* \hat{H}_j(x;A_x) U_{11} &\to -\frac{\hbar^2\partial_x^2}{2m_j}, \\
-U_{22}^* \hat{H}_j^*(x;A_x) U_{22} &\to \frac{\hbar^2\partial_x^2}{2m_j}, \\
\Delta_j(x) U_{11}^* U_{22} &\to \widetilde{\Delta}_j(x),
\end{aligned} \tag{B2}$$

while the BdG state associated with $\widetilde{H}_{BdG}^{(j)}$ is given by $\widetilde{\Psi}_j = U^\dagger\Psi_j$. The pair potential $\widetilde{\Delta}_j(x)$ takes the same mathematical structure as the one presented in Eq. (2), the only action of the unitary transformation being the substitution of the phase difference φ with $\widetilde{\varphi} = \varphi - 2\pi\frac{\Phi}{\Phi_0}\frac{y}{L}$. As a consequence the phase difference between the two sides of the junction is modulated along the junction, and this modulation is the source of the magnetic diffraction pattern affecting the critical current of the junction. Under our assumptions, the y dependence of the pair potential is adiabatic compared to the microscopic scale of the problem. This statement can be rigorously proved using the two-scale perturbation theory [76]. In particular the wave vector, $q = \frac{2\pi}{L}\frac{\Phi}{\Phi_0}$, modulating the superconducting phase is much smaller than the Fermi wave vectors $r_j k_F$, and thus the phase modulation along the y direction enters only parametrically in the one-dimensional problem described in the main text. The validity of these arguments also requires that the Cooper pairs tunneling with normal incidence represent the dominant microscopic process and thus the energy associated with transverse modes is negligible compared to the Fermi energy. When the energy of the transverse modes becomes relevant (e.g., for very short junctions with $L \ll \lambda$) on the Fermi energy scale, a full treatment of the transverse degrees of freedom is required. Hereafter, we focus our attention on the case of adiabatic phase variation of $\widetilde{\varphi}$ along the transverse dimension of the junction. Under this assumption, once the current-phase relation $I_J(\varphi)$ has been obtained according to the procedure given in the main text, the magnetic field dependence of the critical current of the junction is obtained according to the formula

$$I_c(\Phi) = \max_{\varphi\in[0,2\pi]}\int_{-L/2}^{L/2}\frac{dy}{L} I_J\left(\varphi - 2\pi\frac{\Phi}{\Phi_0}\frac{y}{L}\right), \tag{B3}$$

where the current-phase relation presents a parametric dependence on y. A further progress can be done observing that the current-phase relation is an odd function of the

phase difference, and thus it can be written as $I_J(\varphi) = \sum_{n=0}^{\infty} a_n \sin(n\varphi)$. As a consequence, Eq. (B3) takes the form

$$I_c(\Phi) = \max_{\varphi\in[0,2\pi]} \sum_{n=0}^{\infty} a_n \sin(n\varphi) \frac{\sin\left(n\frac{\pi\Phi}{\Phi_0}\right)}{n\frac{\pi\Phi}{\Phi_0}}, \tag{B4}$$

where the coefficients a_n can be directly extracted by $I_J(\varphi)$ using the relation

$$a_n = \frac{1}{\pi}\int_0^{2\pi} I_J(\varphi)\sin(n\varphi)d\varphi, \tag{B5}$$

where we explicitly used the orthogonality condition $\int_0^{2\pi} \sin(n\varphi)\sin(m\varphi)d\varphi = \pi\delta_{n,m}$. Equation (B4) provides the Fraunhofer diffraction pattern,

$$I_c(\Phi)/I_c(0) = \left|\frac{\sin\left(\frac{\pi\Phi}{\Phi_0}\right)}{\frac{\pi\Phi}{\Phi_0}}\right|,$$

when a single-harmonic current-phase dependence $I_J(\varphi) = a_1\sin(\varphi)$ is considered, while deviations are expected if the high-harmonic contribution is not negligible. For the above reasons, the magnetic diffraction pattern $I_c(\Phi)$ is an indirect probe of the harmonic content of the current-phase relation of the junction. Our treatment of the magnetic field effects on the junction justifies the validity of the approach proposed in Refs. [77,78] and the classical argument given in Ref. [75].

[1] H. Suhl, B. T. Matthias, and L. R. Walker, Phys. Rev. Lett. **3**, 552 (1959); V. A. Moskalenko, Fiz. Met. Metalloved. **8**, 503 (1959) [Phys. Met. Metallogr. **8**, 25 (1959)].

[2] J. Bardeen, L. N. Cooper, and J. R. Schrieffer, Phys. Rev. **108**, 1175 (1957).

[3] J. Nagamatsu, N. Nakagawa, T. Muranaka, Y. Zenitani, and J. Akimitsu, Nature (London) **410**, 63 (2001).

[4] Y. Kamihara, T. Watanabe, M. Hirano, and H. Hosono, J. Am. Chem. Soc. **130**, 3296 (2008).

[5] G. R. Stewart, Rev. Mod. Phys. **83**, 1589 (2011).

[6] F. Giubileo, D. Roditchev, W. Sacks, R. Lamy, D. X. Thanh, J. Klein, S. Miraglia, D. Fruchart, J. Marcus, and Ph. Monod, Phys. Rev. Lett. **87**, 177008 (2001).

[7] I. I. Mazin, D. J. Singh, M. D. Johannes, and M. H. Du, Phys. Rev. Lett. **101**, 057003 (2008); K. Kuroki, S. Onari, R. Arita, H. Usui, Y. Tanaka, H. Kontani, and H. Aoki, *ibid.* **101**, 087004 (2008).

[8] R. S. Gonnelli, D. Daghero, G. A. Ummarino, A. Calzolari, M. Tortello, V. A. Stepanov, N. D. Zhigadlo, K. Rogacki, J. Karpinski, F. Bernardini, and S. Massidda, Phys. Rev. Lett. **97**, 037001 (2006).

[9] D. Daghero, M. Tortello, G. A. Ummarino, and R. S. Gonnelli, Rep. Prog. Phys. **74**, 124509 (2011).

[10] W. K. Park, J. L. Sarrao, J. D. Thompson, and L. H. Greene, Phys. Rev. Lett. **100**, 177001 (2008).

[11] S. Kashiwaya, Y. Tanaka, M. Koyanagi, H. Takashima, and K. Kajimura, Phys. Rev. B **51**, 1350 (1995).

[12] T. Y. Chen, Z. Tesanovic, R. H. Liu, X. H. Chen, and C. L. Chien, Nature (London) **453**, 1224 (2008).

[13] X. Lu, W. K. Park, H. Q. Yuan, G. F. Chen, G. L. Luo, N. L. Wang, A. S. Sefat, M. A. McGuire, R. Jin, B. C. Sales, D. Mandrus, J. Gillett, S. E. Sebastian, and L. H. Greene, Supercond. Sci. Technol. **23**, 054009 (2010).

[14] E. Il'ichev, M. Grajcar, R. Hlubina, R. P. J. Ijsselsteijn, H. E. Hoenig, H.-G. Meyer, A. Golubov, M. H. S. Amin, A. M. Zagoskin, A. N. Omelyanchouk, and M. Yu. Kupriyanov, Phys. Rev. Lett. **86**, 5369 (2001).

[15] G. Testa, A. Monaco, E. Esposito, E. Sarnelli, D.-J. Kang, S. H. Mennema, E. J. Tarte, and M. G. Blamire, Appl. Phys. Lett. **85**, 1202 (2004).

[16] G. Testa, E. Sarnelli, A. Monaco, E. Esposito, M. Ejrnaes, D.-J. Kang, S. H. Mennema, E. J. Tarte, and M. G. Blamire, Phys. Rev. B **71**, 134520 (2005).

[17] E. Sarnelli, M. Adamo, S. De Nicola, S. Cibella, R. Leoni, and C. Nappi, Supercond. Sci. Technol. **26**, 105013 (2013).

[18] M. A. N. Araujo and P. D. Sacramento, Phys. Rev. B **79**, 174529 (2009).

[19] J.-B. Xia, Phys. Rev. B **45**, 3593 (1992).

[20] F. Romeo and R. Citro, Phys. Rev. B **91**, 035427 (2015).

[21] C. H. Wu, W. C. Chang, J. T. Jeng, M. J. Wang, Y. S. Li, H. H. Chang, and M. K. Wu, Appl. Phys. Lett. **102**, 222602 (2013).

[22] A. V. Burmistrova and I. A. Devyatov, Europhys. Lett. **107**, 67006 (2014).

[23] A. V. Burmistrova, I. A. Devyatov, A. A. Golubov, K. Yada, and Y. Tanaka, J. Phys. Soc. Jpn. **82**, 034716 (2013).

[24] A. A. Golubov and I. I. Mazin, Appl. Phys. Lett. **102**, 032601 (2013).

[25] C. Nappi, S. De Nicola, M. Adamo, and E. Sarnelli, Europhys. Lett. **102**, 47007 (2013).

[26] A. Moor, A. F. Volkov, and K. B. Efetov, Phys. Rev. B **87**, 100504 (2013).

[27] W. Da, L. Houng-Yan, and W. Qiang-Hua, Chin. Phys. Lett. **30**, 077404 (2013).

[28] V. G. Stanev and A. E. Koshelev, Phys. Rev. B **86**, 174515 (2012).

[29] S. Z. Lin, Phys. Rev. B **86**, 014510 (2012).

[30] S. Apostolov and A. Levchenko, Phys. Rev. B **86**, 224501 (2012).

[31] A. E. Koshelev and V. G. Stanev, Europhys. Lett. **96**, 27014 (2011).

[32] E. Berg, N. H. Lindner, and T. Pereg-Barnea, Phys. Rev. Lett. **106**, 147003 (2011).

[33] Y. Ota, N. Nakai, H. Nakamura, M. Machida, D. Inotani, Y. Ohashi, T. Koyama, and H. Matsumoto, Phys. Rev. B **81**, 214511 (2010).

[34] Yu. Erin and A. N. Omel'yanchuk, Low. Temp. Phys. **36**, 969 (2010).

[35] D. Parker and I. I. Mazin, Phys. Rev. Lett. **102**, 227007 (2009).

[36] J. Wu and P. Phillips, Phys. Rev. B **79**, 092502 (2009).

[37] T. K. Ng and N. Nagaosa, Europhys. Lett. **87**, 17003 (2009).

[38] A. A. Golubov, A. Brinkman, Y. Tanaka, I. I. Mazin, and O. V. Dolgov, Phys. Rev. Lett. **103**, 077003 (2009).

[39] J. Linder, I. B. Sperstad, and A. Sudbø, Phys. Rev. B **80**, 020503(R) (2009).

[40] W.-F. Tsai, D.-X. Yao, B. A. Bernevig, and J. P. Hu, Phys. Rev. B **80**, 012511 (2009).

[41] W.-Q. Chen, F. Ma, Z.-Y. Lu, and F.-C. Zhang, Phys. Rev. Lett. **103**, 207001 (2009).

[42] S. Döring, S. Schmidt, D. Reifert, M. Feltz, M. Monecke, N. Hasan, V. Tympel, F. Schmidl, J. Engelmann, F. Kurth, K. Iida, I. Mönch, B. Holzapfel, and P. Seidel, J. Supercond. Nov. Magn. **28**, 1117 (2015).

[43] S. Döring, S. Schmidt, F. Schmidl, V. Tympel, S. Haindl, F. Kurth, K. Iida, I. Mönch, B. Holzapfel, and P. Seidel, Supercond. Sci. Technol. **25**, 084020 (2012).

[44] S. Döring, M. Monecke, S. Schmidt, F. Schmidl, V. Tympel, J. Engelmann, F. Kurth, K. Iida, S. Haindl, I. Mönch, B. Holzapfel, and P. Seidel, J. Appl. Phys. **115**, 083901 (2014).

[45] S. Schmidt, S. Döring, F. Schmidl, V. Tympel, S. Haindl, K. Iida, F. Kurth, B. Holzapfel, and P. Seidel, IEEE Trans. Appl. Supercond. **23**, 7300104 (2013).

[46] S. Lee, J. Jiang, J. D. Weiss, C. M. Folkman, C. W. Bark, C. Tarantini, A. Xu, D. Abraimov, A. Polyanskii, C. T. Nelson, Y. Zhang, S. H. Baek, H. W. Jang, A. Yamamoto, F. Kametani, X. Q. Pan, E. E. Hellstrom, A. Gurevich, C. B. Eom, and D. C. Larbalestier, Appl. Phys. Lett. **95**, 212505 (2009).

[47] T. Katase, Y. Ishimaru, A. Tsukamoto, H. Hiramatsu, T. Kamiya, K. Tanabe, and H. Hosono, Appl. Phys. Lett. **96**, 142507 (2010).

[48] T. Katase, Y. Ishimaru, A. Tsukamoto, H. Hiramatsu, T. Kamiya, K. Tanabe, and H. Hosono, Supercond. Sci. Technol. **23**, 082001 (2010).

[49] E. Sarnelli, M. Adamo, C. Nappi, V. Braccini, S. Kawale, E. Bellingeri, and C. Ferdeghini, Appl. Phys. Lett. **104**, 162601 (2014).

[50] C. Barone, F. Romeo, S. Pagano, M. Adamo, C. Nappi, E. Sarnelli, F. Kurth, and K. Iida, Sci. Rep. **4**, 6163 (2014).

[51] P. Seidel, Supercond. Sci. Technol. **24**, 043001 (2011).

[52] G. E. Blonder, M. Tinkham, and T. M. Klapwijk, Phys. Rev. B **25**, 4515 (1982).

[53] Observing that $mr_j^2 = m_j$ and $r_j k_F = k_F^{(j)}$, the quantity $r_j Z = \frac{mU_0}{\hbar^2 k_F} r_j$ can be easily identified as the Blonder-Thinkham-Klapwijk parameter describing the scattering of a quasiparticle of mass m_j and wave vector $k_F^{(j)}$, i.e., $Z_j = \frac{m_j U_0}{\hbar^2 k_F^{(j)}}$.

[54] C. W. J. Beenakker, Phys. Rev. Lett. **67**, 3836 (1991).

[55] The first quantization operators $\overleftarrow{\partial}_x$ or $\overrightarrow{\partial}_x$ act over the second quantization fields $\hat{A}$ and $\hat{B}$ as follows: $\hat{A}[\alpha \overrightarrow{\partial}_x + \beta \overleftarrow{\partial}_x]\hat{B} = \alpha \hat{A}(\partial_x \hat{B}) + \beta(\partial_x \hat{A})\hat{B}$, with α, βc numbers.

[56] In the absence of magnetic potentials, the intensity of the charge current $\bar{J}_{ch,\sigma} = \sum_j \langle \hat{\psi}_{j\sigma}^\dagger \check{\mathcal{J}}_j \hat{\psi}_{j\sigma} \rangle$ sustained by spin $\sigma \in \{\uparrow, \downarrow\}$ electrons does not depend on the spin projection σ, i.e., $\bar{J}_{ch,\uparrow} = \bar{J}_{ch,\downarrow}$. As a consequence $\bar{J}_{ch}$ can be computed according to the formula $\bar{J}_{ch} = 2\bar{J}_{ch,\uparrow}$, as performed in the main text.

[57] The charge current $\bar{J}_{ch}$ can be expressed in units of $|e|\Delta_\alpha(0)/\hbar$ according to the formula $\mathcal{I} = 2 \cdot \chi_0^{-1} \sum_j r_j^{-1} u_j v_j k_F^{-1} (|c_j|^2 - |d_j|^2) \tanh[E_B/(2k_B T)]$, with $\bar{J}_{ch} = \frac{|e|\Delta_\alpha(0)}{\hbar}\mathcal{I}$.

[58] A. Furusaki, Superlatt. Microstruct. **25**, 809 (1999).

[59] R. R. Schulz, B. Chesca, B. Goetz, C. W. Schneider, A. Schmehl, H. Bielefeldt, H. Hilgenkamp, J. Mannhart, and C. C. Tsuei, Appl. Phys. Lett. **76**, 912 (1999).

[60] C. C. Tsuei and J. R. Kirtley, Rev. Mod. Phys. **72**, 969 (2000).

[61] C. C. Tsuei and J. R. Kirtley, Phys. Rev. Lett. **85**, 182 (2000).

[62] A. A. Golubov, M. Yu. Kupriyanov, and E. Ilichev, Rev. Mod. Phys. **76**, 411 (2004).

[63] A. H. Silver and J. E. Zimmerman, Phys. Rev. **157**, 317 (1967).

[64] R. Rifkin and B. S. Deaver, Phys. Rev. B **13**, 3894 (1976).

[65] E. Il'ichev, V. Zakosarenko, R. P. J. IJsselsteijn, V. Schultze, H.-G. Meyer, H. E. Hoenig, H. Hilgenkamp, and J. Mannhart, Phys. Rev. Lett. **81**, 894 (1998).

[66] E. Il'ichev, V. Zakosarenko, R. P. J. IJsselsteijn, H. E. Hoenig, H.-G. Meyer, M. V. Fistul, and P. Müller, Phys. Rev. B **59**, 11502 (1999).

[67] E. Il'ichev, V. Zakosarenko, L. Fritzsch, R. Stolz, H. E. Hoenig, H.-G. Meyer, A. B. Zorin, V. V. Khanin, M. Götz, A. B. Pavolotsky, and J. Niemeyer, Rev. Sci. Instrum. **72**, 1882 (2001).

[68] I. Sochnikov, A. J. Bestwick, J. R. Williams, T. M. Lippman, I. R. Fisher, D. Goldhaber-Gordon, J. R. Kirtley, and K. A. Moler, Nano Lett. **13**, 3086 (2013).

[69] A. Moor, A. F. Volkov, and K. B. Efetov, Phys. Rev. B **83**, 134524 (2011).

[70] Y. Tanaka and S. Kashiwaya, Phys. Rev. B **53**, R11957(R) (1996).

[71] Yu. S. Barash, H. Burkhardt, and D. Rainer, Phys. Rev. Lett. **77**, 4070 (1996).

[72] R. A. Riedel and P. F. Bagwell, Phys. Rev. B **57**, 6084 (1998).

[73] A. Brinkman, A. A. Golubov, H. Rogalla, O. V. Dolgov, J. Kortus, Y. Kong, O. Jepsen, and O. K. Andersen, Phys. Rev. B **65**, 180517(R) (2002); A. Brinkman, A. A. Golubov, and M. Yu. Kupriyanov, *ibid.* **69**, 214407 (2004); K. Chen, C. G. Zhuang, Q. Li, Y. Zhu, P. M. Voyles, X. Weng, J. M. Redwing, R. K. Singh, A. W. Kleinsasser, and X. X. Xi, Appl. Phys. Lett. **96**, 042506 (2010).

[74] R. De Luca, Eur. Phys. J. B **86**, 294 (2013), see Eq. (17).

[75] A. Barone and G. Paternò, *Physics and Applications of the Josephson Effect* (John Wiley & Sons, New York, 1982).

[76] S. H. Strogatz, *Nonlinear Dynamics and Chaos: With Applications to Physics, Biology, Chemistry, and Engineering* (Perseus Books, Cambridge, 1994), see Chap. 7.

[77] E. Goldobin, D. Koelle, R. Kleiner, and A. Buzdin, Phys. Rev. B **76**, 224523 (2007).

[78] I. B. Sperstad, J. Linder, and A. Sudbø, Phys. Rev. B **80**, 144507 (2009).